Iranian Journal of Numerical Analysis and Optimization
Vol. 16, No. 4, 2026, pp 1518–1549
https://doi.org/10.22067/ijnao.2026.97820.1844
https://ijnao.um.ac.ir/

Research Article

A collocation framework for numerical reconstruction of the source function in a two-term fractional diffusion problem

S.S. Jalalian, A. Babaei*, and M. Gachpazan

Abstract

This study develops a new spectral collocation strategy to reconstruct an unknown source term appearing in a two-term time-fractional diffusion model equipped with nonlocal boundary constraints. As obtaining an exact solution to such problems is generally intractable, a collocation strategy based on Legendre polynomials and Chebyshev nodes is employed to construct the numerical approximation. By projecting the fractional-order operators onto a bivariate polynomial basis, the original inverse problem is transformed into a system of linear algebraic equations. The solvability of the resulting system is investigated via the properties of the associated collocation matrix incorporating the fractional dynamics and nonlocal boundary

*Corresponding author

Received 13 February 2026; revised 26 May 2026; accepted 25 June 2026

Sahar Jalalian
Department of Applied Mathematics, Faculty of Mathematical Sciences, University of Mazandaran, Babolsar, Iran. e-mail: s.jalalian01@umail.umz.ac.ir

Afshin Babaei
Department of Applied Mathematics, Faculty of Mathematical Sciences, University of Mazandaran, Babolsar, Iran. e-mail: babaei@umz.ac.ir

Mortaza Gachpazan
Department of Applied Mathematics, Faculty of Mathematical Sciences, Ferdowsi University of Mashhad, P. O. Box 1159, Mashhad 91755, Iran. e-mail: gachpazan@um.ac.ir

How to cite this article
Jalalian, S.S., Babaei, A. and Gachpazan, M., A collocation framework for numerical reconstruction of the source function in a two-term fractional diffusion problem. *Iran. J. Numer. Anal. Optim.*, 2026; 16(4): 1518-1549. https://doi.org/10.22067/ijnao.2026.97820.1844

conditions. Moreover, convergence analysis and rigorous error estimates are provided. Numerical trials are presented to demonstrate the reliability, precision, and computational efficiency of the proposed procedure.

AMS subject classifications (2020): Primary 35R30; Secondary 65M32, 65M12.

Keywords: Fractional diffusion equation; Inverse source problem; Nonlocal boundary conditions; Error analysis.

1 Introduction

Recent developments in the analysis of inverse and ill-posed problems have increasingly focused on boundary conditions of a nonlocal nature. Rather than prescribing data solely at the boundary, these conditions utilize integral operators or global solution information, capturing situations in which physical observations along the boundary cannot be directly accessed. This generality, however, introduces significant challenges for both mathematical analysis and numerical computation [38].

The applicability of nonlocal boundary value problems spans a diverse range of scientific and engineering fields. These problems are crucial for modeling phenomena characterized by long-range interactions, memory effects, or integral constraints, where traditional local models prove insufficient. Key applications include thermal distributions in composite materials and cables, resistivity well-logging in geophysics, biological tissue dynamics, and medical imaging techniques such as ultrasound [32, 14, 36, 29, 27, 21]. Furthermore, these conditions arise naturally in models of multiphase flow, where the heat flux between phases depends on spatially and temporally varying parameters, thereby reflecting complex interfacial interactions [26, 43]. The advent of fractional-order differential equations, which inherently capture nonlocal temporal and spatial effects, has further underscored the importance of such problems [41, 27, 35].

Numerous computational techniques have been developed to solve these inverse problems, often combining rigorous mathematical theory with practical algorithms such as regularization and iterative projection methods [42, 9, 3]. Recent advances have also begun to incorporate data-driven and machine learning approaches to further enhance accuracy and efficiency [3].

A classical and extensively studied inverse problem is that of determining the heat source under nonlocal boundary conditions. For instance, models involving uncertain coefficients and time-dependent sources subject to integral over-determination, motivated by applications in mathematical biology, have been investigated in [33, 17]. Analytical approaches, including generalized

Fourier series expansions, have been employed to establish uniqueness, solvability, and stability results. Similarly, the field of fractional calculus has attracted considerable attention. Works such as [24, 1, 30, 16, 2] address time- and space-dependent source functions in fractional parabolic models, while studies such as [20, 18, 4] focus on heat equations with Wentzell-Neumann-type boundary conditions and integral constraints, proposing both theoretical and numerical solutions. Inverse problems for fractional diffusion and subdiffusion models involving Caputo or generalized fractional derivatives have also received considerable attention. Unique solvability under suitable over-determination conditions has been established in [25], while extensions to multi-term and sequential fractional derivatives have been analyzed in [22, 6, 28, 7, 15]. These studies address numerical stability and nonlinear cases through iterative and matrix-based techniques. Moreover, substantial research has been devoted to problems for equations featuring multiple fractional time derivatives, including fractional telegraph, diffusion, and wave equations [5, 8, 10, 11, 34, 39, 40, 44].

Recent studies have explored inverse source problems for diffusion equations involving two-term time-fractional derivatives with nonlocal boundary specifications. Notably, in [12] and [13], the existence, uniqueness, and well-posedness of such problems have been established using analytical approaches, such as the generalized Fourier method. While these works provide a solid theoretical foundation, their practical implementation often requires complex problem decomposition into multiple sub-problems and extensive analytical expansions, which can be computationally intensive for applied scenarios.

To address these limitations, the present work develops a more direct and computationally efficient numerical framework based on the shifted Legendre-Chebyshev spectral collocation method. Unlike the existing analytical splitting techniques, our approach offers a unified scheme that handles multi-term fractional derivatives and nonlocal constraints simultaneously without the need for problem decomposition. The primary innovations and contributions of this study are as follows: (i) the development of a straightforward collocation scheme that simplifies the numerical treatment of multi-term fractional inverse problems; (ii) the provision of a highly accurate, high-order reconstruction of the unknown source term with reduced overhead; and (iii) demonstrating the robustness and stability of the method even in the presence of noise in the measured data.

The paper is arranged as follows: Section 2 provides the formal statement of the inverse source problem. Section 3 reviews the required background material and definitions. The computational scheme is developed in Section 4. Section 5 contains the error and convergence analysis. Numerical results and discussions are presented in Section 6.

2 Description of the problem

The present work is devoted to an inverse source identification problem for a time-fractional diffusion equation involving two distinct fractional time derivatives, expressed as

$$D_t^{\alpha} u(x,t) + D_t^{\beta} u(x,t) = u_{xx}(x,t) + r(t)f(x), \qquad (x,t) \in \Omega, \tag{1}$$

for orders $0 < \alpha, \beta < 1$, subject to the initial and nonlocal boundary conditions:

$$u(x,0) = u_0(x), \qquad 0 \le x \le 1, \tag{2}$$

$$au(0,t) + bu(1,t) = 0, \quad 0 \le t \le 1, \tag{3}$$

$$u_x(0,t) - u_x(1,t) + cu(0,t) + du(1,t) = 0, \quad 0 \le t \le 1, \tag{4}$$

where $\Omega = (0,1) \times (0,1]$. In (1), $r(t)f(x)$ is the source function. The constants a, b, c, and d are real numbers with the assumption $a - b \neq 0$.

The operator D_t^{θ} denotes the Caputo fractional derivative defined as [23]

$$D_t^{\theta} u(t) = \frac{1}{\Gamma(1-\theta)} \int_0^t \frac{\partial u(x,s)}{\partial s} \frac{ds}{(t-s)^{\theta}}, \qquad 0 < \theta < 1,$$

where $0 < \theta < 1$ is the derivative order and $\Gamma(\cdot)$ is the Gamma function. For the direct problem associated with (1)–(4), the solution u is sought in Ω such that for each $t \in (0,1)$, $u(\cdot,t)$ belongs to the Sobolev space $H^2[0,1]$ and $D_t^{\alpha} u(x,\cdot), D_t^{\beta} u(x,\cdot)$ are in $C(0,1]$, given a continuous initial temperature u_0 and a continuous source function $r(t)f(x)$.

When the function $r(t)$ is unknown, an inverse problem is formulated to find the pair of functions $\{u(x,t), r(t)\}$ satisfying (1)–(4). To this end, we consider the supplementary integral condition:

$$\int_0^1 u(x,t)\, dx = E(t), \quad 0 \le t \le 1. \tag{5}$$

This form of supplementary condition is utilized when boundary data cannot be measured directly, yet an integral mean of the solution is accessible [19]. The well-posedness of this problem, including the existence, uniqueness, and stability of the solution, has been rigorously established in [12]. In this framework, we seek the pair (u, r) such that $u(\cdot,t) \in H^2[0,1]$ and $r(t) \in C[0,1]$. The use of Sobolev spaces is essential here to provide a rigorous framework and to justify the convergence rates of the numerical method discussed in Section 5. Its fractional derivatives $D_t^{\alpha} u, D_t^{\beta} u \in C(0,1]$. Furthermore, we impose $\int_0^1 f(x)dx \neq 0$ to ensure that the unknown $r(t)$ is uniquely and stably determined.

To solve the inverse problem (1)–(5), we first determine the function $r(t)$. This is achieved by integrating both sides of (1) over $[0, 1]$, with respect to x, yielding

$$\int_0^1 D_t^{\alpha} u(x,t)\,dx + \int_0^1 D_t^{\beta} u(x,t)\,dx = \int_0^1 u_{xx}(x,t)\,dx + r(t)\int_0^1 f(x)\,dx.$$

Since the fractional derivative and the integration act on different variables, the operations are commutative. This leads to

$$D_t^{\alpha}\int_0^1 u(x,t)\,dx + D_t^{\beta}\int_0^1 u(x,t)\,dx = u_x(1,t) - u_x(0,t) + r(t)\int_0^1 f(x)\,dx. \tag{6}$$

We now incorporate information from the boundary conditions (3)–(4) and the supplementary condition (5), obtaining the following relations:

$$\begin{aligned}
&u_x(1,t) - u_x(0,t) = cu(0,t) + du(1,t),\\
&D_t^{\alpha}\int_0^1 u(x,t)\,dx = D_t^{\alpha}E(t),\\
&D_t^{\beta}\int_0^1 u(x,t)\,dx = D_t^{\beta}E(t).
\end{aligned}$$

Substituting these relations into (6) allows us to express $r(t)$ explicitly:

$$r(t) = (\int_0^1 f(x)\,dx)^{-1}(D_t^{\alpha}E(t) + D_t^{\beta}E(t) - (cu(0,t) + du(1,t))). \tag{7}$$

Substituting the expression for $r(t)$ from (7) back into (1) reformulates the original equation into

$$\begin{aligned}
&D_t^{\alpha}u(x,t) + D_t^{\beta}u(x,t)\\
&= u_{xx}(x,t)\\
&\quad + f(x)\left[(\int_0^1 f(x)\,dx)^{-1}(D_t^{\alpha}E(t) + D_t^{\beta}E(t) - (cu(0,t) + du(1,t)))\right].
\end{aligned} \tag{8}$$

Consequently, instead of solving the inverse problem (1)–(5), we can now focus on solving the direct problem defined by (8) subject to the conditions (2)–(4), which is known to be well-posed and possesses a unique solution.

Remark 1. It should be noted that the theoretical well-posedness of this class of inverse fractional source problems, namely existence, uniqueness, and stability with respect to the input data, has been proved in [12]. Hence, the numerical method developed in this work relies on a sound analytical foundation.

3 Preliminaries

This section outlines the essential definitions and preliminary concepts employed in this work.

Definition 1. [31] The Legendre polynomials are defined by the recurrence relation:

$$L_{m+1}(t) = \frac{2m+1}{m+1} t L_m(t) - \frac{m}{m+1} L_{m-1}(t), \qquad m = 1, 2, \ldots,$$

where $L_0(t) = 1$ and $L_1(t) = t$. By applying the variable transformation $t = 2x-1$, and assuming $p_0(x) = 1$ and $p_1(x) = 2x - 1$, the shifted Legendre polynomials $p_m(x),\ m = 1, 2, \ldots$, on the interval $[0, 1]$ are given by the recurrence relation:

$$p_{m+1}(x) = \frac{2m+1}{m+1}(2x-1)p_m(x) - \frac{m}{m+1} p_{m-1}(x).$$

These polynomials satisfy the following orthogonality property:

$$\int_0^1 p_m(x) p_n(x)\, dx = \begin{cases} \frac{1}{2n+1}, & m = n, \\ 0, & m \neq n. \end{cases}$$

The analytical expression for shifted Legendre polynomials is

$$p_n(x) = \sum_{j=0}^{n} (-1)^{n+j} \frac{(n+j)!}{(n-j)!(j!)^2} x^j,$$

Furthermore, $|p_n(x)| \leq 1$ for any $x \in [0, 1]$, and the bound for the m-th derivative is defined by

$$|p_n^{(m)}(x)| \leq m! \frac{(n+m)!}{(n-m)!(m!)^2}, \tag{9}$$

Additionally, these polynomials can be formulated via the Rodrigues formula on the interval $[0, 1]$ as follows:

$$p_m(x) = \frac{1}{m!} \frac{d^m}{dx^m}((x^2 - x)^m).$$

Let $L^2[0, 1]$ denote the Hilbert space of square-integrable functions on the unit interval. Any function $g \in L^2[0, 1]$ admits the orthogonal expansion $g(x) = \sum_{i=0}^{\infty} c_i p_i(x)$, with coefficients c_i obtained from

$$c_i = \frac{1}{\|p_i\|^2} \int_0^1 g(x) p_i(x)\, dx = (2i+1) \int_0^1 g(x) p_i(x)\, dx.$$

Definition 2. [37] Chebyshev polynomials form a sequence of orthogonal polynomials defined on the interval $[-1, 1]$ with respect to particular weight functions. They are classified into two main types: Chebyshev polynomials of the first kind, denoted by $T_n(x)$, satisfying the identity

$$T_n(\cos\theta) = \cos(n\theta), \quad n = 0, 1, 2, \dots,$$

whereas those of the second kind, denoted by $U_n(x)$, are characterized by

$$U_n(\cos\theta)\sin\theta = \sin((n+1)\theta), \quad n = 0, 1, 2, \dots.$$

These polynomials are crucial in approximation theory for minimizing interpolation errors and are widely used in numerical methods.

In this paper, we will utilize the roots of the shifted Chebyshev polynomials of the second kind as collocation points to enhance the accuracy of our method. The shifted roots on $[0, 1]$ are given by

$$t_k = \frac{1}{2}\cos(\frac{k\pi}{n+1}) + \frac{1}{2}, \quad k = 1, \dots, n.$$

4 Numerical Procedure

This section outlines a numerical scheme for addressing problem (8), subject to the conditions (2)–(4). Building upon the findings from the preceding subsection, we proceed to solve (8). For this purpose, we assume an approximate solution of the form:

$$u(x,t) \simeq \tilde{u}_{M,N}(x,t) = \sum_{i=0}^{N}\sum_{j=0}^{M} c_{ij} p_i(x) p_j(t) = P(x)^T C P(t), \tag{10}$$

where $P(x) = [p_0(x), \dots, p_i(x), \dots, p_N(x)]^T, P(t) = [p_0(t), \dots, p_j(t), \dots, p_M(t)]^T$ are vectors of the shifted Legendre polynomials. The unknown coefficients c_{ij} form an $(N+1)\times(M+1)$ matrix C that must be determined through the numerical scheme:

$$C = \begin{bmatrix} c_{0,0} & \cdots & c_{0,M} \\ \vdots & \ddots & \vdots \\ c_{N,0} & \cdots & c_{N,M} \end{bmatrix}.$$

Using conditions (2)-(4) and the governing equation (8), we derive the following relation:

$$\begin{aligned} &P(x)^T C D_t^{\alpha} P(t) + P(x)^T C D_t^{\beta} P(t) \\ &= P_{xx}^T(x) C P(t) \end{aligned} \tag{11}$$

$$+\frac{f(x)}{\int_0^1 f(x)dx}\left[(D_t^{\alpha}E(t)+D_t^{\beta}E(t)-(cP(0)^TCP(t)+dP(1)^TCP(t))\right],$$

where $D_t^{\alpha}P(t)$ and $D_t^{\beta}P(t)$ denote the Caputo fractional derivatives of the vector $P(t)$. These derivatives are defined element-wise, using the formula $D_t^s(t^k)=\frac{\Gamma(k+1)}{\Gamma(k+1-s)}t^{k-s}$, $k\geq 1$ and $0<s<1$. The vector $P_{xx}(x)$ is defined as $P_{xx}=\frac{d^2}{dx^2}P(x)=[\frac{d^2}{dx^2}p_0(x),\dots,\frac{d^2}{dx^2}p_i(x),\dots,\frac{d^2}{dx^2}p_N(x)]^T$. The initial and boundary conditions become

$$P(x)^TCP(0)=u_0(x), \tag{12}$$
$$aP(0)^TCP(t)+bP(1)^TCP(t)=0, \tag{13}$$
$$P_x(0)^TCP(t)-P_x(1)^TCP(t)+cP(0)^TCP(t)+dP(1)^TCP(t)=0, \tag{14}$$

for $0<x<1$ and $0\leq t\leq 1$, where the boundary vectors are defined as follows:

$$P_x(0)=\left[\frac{d}{dx}p_0(0),\dots,\frac{d}{dx}p_i(0),\dots,\frac{d}{dx}p_N(0)\right]^T,$$
$$P_x(1)=\left[\frac{d}{dx}p_0(1),\dots,\frac{d}{dx}p_i(1),\dots,\frac{d}{dx}p_N(1)\right]^T,$$
$$P(0)=\left[p_0(0),\dots,p_N(0)\right],$$
$$P(1)=\left[p_0(1),\dots,p_N(1)\right].$$

Let the spatial collocation nodes x_i, for $i=0,1,\dots,N$, be chosen such that $x_0=0$, $x_N=1$, and $\{x_i : i=1,2,\dots,N-1\}$ are the roots of the second-kind shifted Chebyshev polynomial $U_{N-1}(x)$. The temporal nodes $\{t_j : j=1,2,\dots,M\}$ are chosen as the roots of $U_M(t)$. Collocating (11) at the $M\times(N-1)$ points (x_i,t_j) yields

$$\begin{aligned}&P(x_i)^TCD_t^{\alpha}P_(t_j)+P(x_i)^TCD_t^{\beta}P(t_j)\\&=P_{xx}(x_i)^TCP(t_j)\\&+\frac{f(x_i)}{(\int_0^1 f(x)dx)}\left[\left(D_t^{\alpha}E(t_j)+D_t^{\beta}E(t_j)-(cP(0)^TCP(t_j)+dP(1)^TCP(t_j))\right)\right].\end{aligned} \tag{15}$$

The initial condition (12) is collocated at the spatial nodes $x_i,\ i=0,1,\dots,N$, as

$$P(x_i)CP(t=0)=u_0(x_i). \tag{16}$$

Also, the boundary conditions (13)–(14) are collocated at the temporal nodes $t_j,\ j=1,\dots,M$,

$$aP(0)^T CP(t_j) + bP(1)CP(t_j) = 0, \tag{17}$$

$$P_x(0)^T CP(t_j) - P_x(1)^T CP(t_j) + cP(0)^T CP(t_j) + dP(1)^T CP(t_j) = 0. \tag{18}$$

To streamline the discrete formulation, we introduce the following auxiliary matrices and vectors:

Spatial matrices

(each of size $(N-1) \times (N+1)$)

$$A_{11} = \Big[P(x_1) \cdots P(x_{N-1})\Big]^T,$$

$$A_{12} = \Big[P_{xx}(x_1) \cdots P_{xx}(x_{N-1})\Big]^T.$$

Temporal matrices

(each of size $(M+1) \times M$)

$$A_{13} = \big[D_t^{\alpha} P(t_1) \ \cdots \ D_t^{\alpha} P(t_M)\big],$$

$$A_{14} = \big[D_t^{\beta} P(t_1) \ \cdots \ D_t^{\beta} P(t_M)\big],$$

$$A_{15} = \big[P(t_1) \ \cdots \ P(t_M)\big].$$

Forcing vectors

$$F = \left(\int_0^1 f(x)\, dx\right)^{-1} \begin{bmatrix} f(x_1) \\ \vdots \\ f(x_{N-1}) \end{bmatrix} \quad \text{(size } (N-1) \times 1),$$

$$A_{16} = \begin{bmatrix} D_t^{\alpha} E(t_1) \\ \vdots \\ D_t^{\alpha} E(t_M) \end{bmatrix}, \qquad A_{17} = \begin{bmatrix} D_t^{\beta} E(t_1) \\ \vdots \\ D_t^{\beta} E(t_M) \end{bmatrix} \quad \text{(each of size } M \times 1).$$

Using Kronecker product properties, the system (15) can be expressed compactly as follows:

$$\Lambda_1 X = F_1, \tag{19}$$

where $X = [c_{00}, c_{10}, \dots, c_{N0}, \dots, c_{0M}, c_{1M}, \dots, c_N M]^T$ is the vector of unknown coefficients, $\Lambda_1 = A_1 + A_2$, and

$$A_1 = A_{13}^T \otimes A_{11} + A_{14}^T \otimes A_{11} - A_{15}^T \otimes A_{12},$$
$$A_2 = F(c\, A_{15}^T \otimes P(0)^T + d\, A_{15}^T \otimes P(1)^T).$$

Also, $F_1 = F \otimes (A_{16} + A_{17})$. Similarly, the conditions (16)–(18) can be written as follows:

$$\begin{aligned} \Lambda_2 X &= F_2, \\ \Lambda_3 X &= 0, \\ \Lambda_4 X &= 0, \end{aligned} \tag{20}$$

where

$$\begin{aligned} \Lambda_2 &= P(0)^T \otimes A_3, \\ \Lambda_3 &= aA_4^T \otimes P(0)^T + bA_4^T \otimes P(1)^T, \\ \Lambda_4 &= A_4^T \otimes P_x(0)^T - A_4^T \otimes P_x(1)^T + cA_4^T \otimes P(0)^T + dA_4^T \otimes P(1)^T, \\ A_3 &= [P(x_1) \cdots P(x_{N-1})]^T, \\ A_4 &= [P(t_0) \cdots P(t_j) \cdots P(t_M)]^T, \end{aligned}$$

and $F_2 = [U_0(x_1) \cdots U_0(x_{N-1})]^T$. Combining (19) and (20) results in a linear system of $(N+1)(M+1)$ equations as follows:

$$AX = \digamma, \tag{21}$$

where $A = [\Lambda_1^T, \Lambda_2^T, \Lambda_3^T, \Lambda_4^T]^T$ and $\digamma = [F_1^T, F_2^T, 0, 0]^T$. Solving this linear system (21) for the vector X determines the coefficients c_{ij}. Substituting these coefficients into (10) yields the approximate numerical solution $\tilde{u}_{M,N}(x,t)$.

The transformation of the inverse problem into the algebraic system (21) is theoretically justified through the spectral projection of the fractional-order operators onto the space of shifted Legendre polynomials. Since the basis functions $\{p_i(t)\}_{i=0}^N$ are linearly independent, the resulting discrete formulation provides a valid finite-dimensional representation of the continuous problem. The use of Chebyshev nodes as collocation points yields a stable distribution of nodes, which improves the conditioning of the resulting matrix A and helps mitigate numerical instabilities, including the Runge phenomenon, by increasing node density near the boundaries. The existence of a unique numerical solution X is ensured whenever the collocation matrix A is nonsingular.

5 Error analysis

In this section, we study the convergence of the numerical solution (21) and discuss the stability features of the proposed method.

To investigate the convergence of the proposed approach, we require additional information about the properties of Legendre polynomials, which can be expressed as lemmas and theorems.

Lemma 1. Let $i, j \in \mathbb{N}$, and let $i > j$. Then, for any constant $\theta \geq 1$, the following inequality holds:

$$\frac{i!}{(2i)!} < \theta \frac{j!}{(2j)!}. \tag{22}$$

Proof. Consider the ratio of successive terms. For any positive integer k, we have

$$\frac{\frac{(k+1)!}{(2(k+1))!}}{\frac{k!}{(2k)!}} = \frac{(k+1)!}{k!} . \frac{(2k)!}{(2k+2)!} = (k+1). \frac{1}{2(k+1)(2k+1))} = \frac{1}{2(2k+1)}.$$

Since $k \geq 1$, it follows that $\frac{1}{2(2k+1)} \leq \frac{1}{6} < 1$. Therefore, the sequence $\{\frac{k!}{(2k)!}\}_{k=1}^{\infty}$ is strictly decreasing. Consequently, for any $i > j$, we have

$$\frac{i!}{(2i)!} < \frac{j!}{(2j)!}.$$

□

Theorem 1. Let $f \in C[0,1]$ be such that its derivatives of all orders $i \geq 3$ exist and are uniformly bounded on $[0,1]$, that is,

$$|f^{(i)}(t)| \leq L \quad \text{for all } \ t \in [0,1], \quad \text{for all } \ i \geq 3, \tag{23}$$

where $L > 0$ is a constant independent of i and t. Suppose that $f(t)$ is expanded in the series of shifted Legendre polynomials as

$$f(t) = \sum_{i=0}^{\infty} c_i p_i(t),$$

then, for all $i > 3$, the coefficients satisfy

$$|c_i| \leq L \frac{i!}{(2i)!}. \tag{24}$$

Proof. The proof relies on the Rodrigues formula for shifted Legendre polynomials on $[0,1]$, namely

$$p_i(t) = \frac{1}{i!}\frac{d^i}{dt^i}\Big[t^i(1-t)^i\Big], \quad i = 0, 1, 2, \ldots. \tag{25}$$

A classical result for (shifted) Legendre expansions states that the coefficient c_i in the series

$$f(t) = \sum_{i=0}^{\infty} c_i p_i(t)$$

can be expressed directly in terms of the i-th derivative of f at a specific point. This expression is obtained by repeated integration by parts applied to the orthogonality relation, yielding the identity

$$c_i = (-1)^i \frac{2i+1}{i!}\int_0^1 f^{(i)}(t)(t(1-t))^i\,dt.$$

This identity leverages the fact that the i-th derivative of the shifted Legendre polynomial $p_i(t)$ is a constant, specifically $\frac{(2i)!}{i!}$, and the Rodrigues formula. Taking the absolute value and using the integral inequality, we get

$$|c_i| = |\frac{2i+1}{i!}\int_0^1 f^{(i)}(t)(t(1-t))^i\,dt| \le \frac{2i+1}{i!}\max_{t\in[0,1]}|f^{(i)}|\int_0^1 (t(1-t))^i\,dt.$$

The integral $\int_0^1 (t(1-t))^i\,dt$ is the Beta integral, which evaluates to

$$\int_0^1 (t(1-t))^i\,dt = \beta(i+1, i+1) = \frac{(i!)^2}{(2i+1)!}.$$

Substituting this back into the inequality yields

$$\begin{aligned}
|c_i| &\le \frac{2i+1}{i!}\max_{t\in[0,1]}|f^{(i)}(t)|\frac{(i!)^2}{(2i+1)!}\\
&= \max_{t\in[0,1]}|f^{(i)}(t)|\frac{(2i+1)(i!)^2}{i!(2i+1)!}\\
&= \max_{t\in[0,1]}|f^{(i)}(t)|\frac{i!}{(2i)!}.
\end{aligned}$$

So, we have

$$|c_i| \le \max_{t\in[0,1]}|f^{(i)}(t)|\frac{i!}{(2i)!}.$$

For $i \ge 3$, under the given smoothness conditions, $\max_{t\in[0,1]}|f^{(i)}(t)|$ can be bounded by a constant L. For sufficiently large i, this implies the desired bound. Hence, for all $i > 3$, we obtain the desired bound:

$$|c_i| \le L\frac{i!}{(2i)!}$$

for all $i > 3$, which completes the proof. According to Lemma 1, this bound decreases rapidly as i increases, ensuring the convergence of the approximate solution. $\square$

It is worth noting that while the estimate in (22) exhibits factorial decay —reflecting the behavior for analytic or highly smooth functions— this serves as an upper bound for the ideal case. For solutions with limited regularity (e.g., in Sobolev spaces H^k), this bound naturally transitions to a standard algebraic rate, $\mathcal{O}(N^{-k})$. However, to maintain the consistency of the theoretical framework presented in this section, we present the estimates in their strongest form.

Theorem 2. Let $f_N(t) = \sum_{i=0}^{N} c_i p_i(t)$ be an approximation of $f(t)$. Then

$$|f(t) - f_N(t)| \leq \frac{L}{(N+1)!}. \tag{26}$$

Proof. We know from standard approximation theory that

$$|f(t) - f_N(t)| \leq \frac{1}{(N+1)!} \max_{0\leq t\leq 1} f^{(N+1)}(t)$$

It can be shown that for the specific basis functions $p_i(t)$,

$$f^{(N+1)}(t) = c_{N+1}\left(\frac{(2N+2)!}{((N+1)!)^2}(N+1)!\right) = \frac{(2N+2)!}{(N+1)!}c_{N+1}.$$

Applying (24), c_{N+1} can be bounded as $c_{N+1} \leq \frac{(N+1)!}{(2N+2)!}$, therefore

$$|f(t) - f_N(t)| \leq L\frac{1}{(N+1)!}.$$

$\square$

Now, consider a bivariate function

$$f(x,t) = \sum_{i=0}^{\infty}\sum_{j=0}^{\infty} c_{ij} p_i(x) p_j(t).$$

Suppose

$$\|\frac{\partial^{i+j} f(x,t)}{\partial x^i \partial t^j}\|_2 \leq \eta,$$

for a positive constant η. Then, the following inequality holds for the expansion coefficients $c_{i,j}$:

$$|c_{i,j}| < \eta \frac{i!\, j!}{(2i)!\,(2j)!}, \tag{27}$$

for all $i, j > 3$. Furthermore, if $\tilde{f}(x,t) = \sum_{i=0}^{N} \sum_{j=0}^{M} c_{i,j} p_i(x) p_j(t)$ is an approximation of $f(x,t)$, then we have

$$|f(x,t) - \tilde{f}(x,t)| < \frac{\eta}{(N+1)!(M+1)!}. \tag{28}$$

The following lemma confirms the validity of inequalities essential for deriving this error estimate.

Lemma 2. Let $f(x,t)$ and its approximation $\tilde{f}(x,t)$ satisfy the assumptions of Theorem 2 and its consequence (28). Then there exists a positive constant η, independent of the discretization parameters, such that the following error estimates hold:

(i)

$$\left| \frac{\partial f(x,t)}{\partial x} - \frac{\partial \tilde{f}(x,t)}{\partial x} \right| < \frac{\eta}{2N^{N-1} M^{M+1}},$$

(ii)

$$\left| \frac{\partial^2 f(x,t)}{\partial x^2} - \frac{\partial^2 \tilde{f}(x,t)}{\partial x^2} \right| < \frac{\eta}{4N^{N-2} M^{M+1}},$$

(iii)

$$\left| D_t^{\alpha} f(x,t) - D_t^{\alpha} \tilde{f}(x,t) \right| < \frac{\eta}{N^{N-1} M^{M+1}}.$$

Proof. (i) From the definition of $f(x,t)$ and $\tilde{f}(x,t)$, we have

$$\left| \frac{\partial f(x,t)}{\partial x} - \frac{\partial \tilde{f}(x,t)}{\partial x} \right| = |\sum_{i=N+1}^{\infty} \sum_{j=M+1}^{\infty} c_{i,j} p_i'(x) p_j(t)|.$$

This can be bounded by

$$\left| \frac{\partial f(x,t)}{\partial x} - \frac{\partial \tilde{f}(x,t)}{\partial x} \right| \leq \sum_{i=N+1}^{\infty} \sum_{j=M+1}^{\infty} |c_{i,j}||p_i'(x)||p_j(t)|.$$

Given that $|p_j(t)| \leq 1$ on $[0,1]$ and applying the coefficient bound from (27), this inequality becomes

$$\sum_{i=N+1}^{\infty} \sum_{j=M+1}^{\infty} |c_{i,j}||p_i'(x)||p_j(t)| \leq \sum_{i=N+1}^{\infty} \sum_{j=M+1}^{\infty} (\eta \frac{i!\, j!}{(2i)!(2j)!}) |p_i'(x)|.$$

From property (9), we use the bound $|p_i'(x)| \leq \frac{(i+1)!}{(i-1)!}$ for $x \in [0,1]$. Substituting this yields

$$|\frac{\partial f(x,t)}{\partial x} - \frac{\partial \tilde{f}(x,t)}{\partial x}| \leq \sum_{i=N+1}^{\infty} \sum_{j=M+1}^{\infty} (\frac{\eta i! j!}{(2i)!(2j)!})(\frac{(i+1)!}{(i-1)!}).$$

Therefore, considering the above relationship and the properties of geometric series, we can write

$$\begin{aligned}
&\eta \sum_{i=N+1}^{\infty} (\frac{i!}{(2i)!})(\frac{(i+1)!}{(i-1)!}) \sum_{j=M+1}^{\infty} (\frac{j!}{(2j)!})\\
&\leq \frac{\eta}{2}(\sum_{i=N+1}^{\infty} \frac{1}{i^{i-2}})(\sum_{j=M+1}^{\infty} \frac{1}{j^j})\\
&\leq (\frac{\eta}{2})(\sum_{i=N+1}^{\infty} (\frac{1}{N+1})^{i-2})(\sum_{j=M+1}^{\infty} (\frac{1}{M+1})^{j})\\
&= \frac{\eta}{2N(N+1)^(N-2)M(M+1)^M} \leq \frac{\eta}{2N^{N-1}M^{M+1}}.
\end{aligned}$$

So, we obtain the final bound:

$$\left| \frac{\partial f(x,t)}{\partial x} - \frac{\partial \tilde{f}(x,t)}{\partial x} \right| < \frac{\eta}{2N^{N-1}M^{M+1}}.$$

(ii) The proof for the second derivative follows similarly, using the bound $|p_i''(x)| \leq \frac{(i+2)!}{2(i-2)!} \leq \frac{(i+2)!}{(i-2)!}$ and the same coefficient bound (27). This leads to

$$\left| \frac{\partial^2 f(x,t)}{\partial x^2} - \frac{\partial^2 \tilde{f}(x,t)}{\partial x^2} \right| \leq \frac{\eta}{4N^{N-2}M^{M+1}}.$$

(iii) For the Caputo fractional derivative, we use the linearity property and the fact that $D_t^\alpha(t^k) = \frac{\Gamma(k+1)}{\Gamma(k+1-\alpha)} t^{k-\alpha}$. The error bound is derived by applying the same coefficient bound and the properties of Gamma function, yielding

$$\begin{aligned}
\left| D_t^\alpha f(x,t) - D_t^\alpha \tilde{f}(x,t) \right| &= |\frac{1}{\Gamma(1-\alpha)} \int_0^t (t-s)^{-\alpha} (\frac{d}{ds}(f(x,t) - \tilde{f}(x,t)))ds|\\
&\leq \frac{1}{|\Gamma(1-\alpha)|} \int_0^1 |(1-s)|^{-\alpha} |\frac{\partial}{\partial s}((f(x,s) - \tilde{f}(x,s))|\, ds.
\end{aligned}$$

Applying the bound from part (i) to the derivative, which is independent of s, we get

$$\left| D_t^\alpha f(x,t) - D_t^\alpha \tilde{f}(x,t) \right| \leq (\frac{1}{|\Gamma(1-\alpha)|})(\frac{\eta}{2N^{N-1}M^{M+1}}) \int_0^t (1-s)^{-\alpha}\, ds.$$

Evaluating the integral yields

$$\left| D_t^\alpha f(x,t) - D_t^\alpha \tilde{f}(x,t) \right| \leq (\frac{\eta}{|\Gamma(2-\alpha)| 2N^{N-1}M^{M+1}}).$$

Since $|\Gamma(2-\alpha)|$ is a positive constant for $\alpha \in (0,1)$, it can be absorbed into the constant η, yielding the final result:

$$\left|D_t^{\alpha} f(x,t) - D_t^{\alpha} \tilde{f}(x,t)\right| \leq \frac{\eta}{N^{N-1} M^{M+1}}.$$

Thus, the proof of the lemma is complete. □

Theorem 3. Let $u(x,t)$ be the exact solution of (1) and let $\tilde{u}(x,t)$ be the approximate solution produced by the present scheme. Assuming the conditions of Lemma 2 are fulfilled, the global truncation error admits the following uniform estimate:

$$\begin{aligned}&\sup_{(x,t)\in\Omega} |u(x,t) - \tilde{u}(x,t)| \\ &< \frac{\eta}{2^{N+M}(N+1)!(M+1)!} + (\|A\|_2)^{-1}(\sqrt{NM})(\frac{3\eta}{N^{N-2}M^{M+1}} + \theta\frac{\vartheta(c+d)}{(M+1)!}).\end{aligned}$$

Proof. Let $g(x,t)$ denote the bivariate interpolating polynomial of the exact solution $u(x,t)$ constructed at the nodal points (x_i, t_j). Here x_i $(i = 0, 1, \ldots, N)$ and $t_j (j = 0, 1, 2, \ldots, M)$ correspond to the roots of the shifted second-kind Chebyshev polynomial within the domain Ω. Applying the triangle inequality yields:

$$|u(x,t) - \tilde{u}(x,t)| \leq |u(x,t) - g(x,t)| + |g(x,t) - \tilde{u}(x,t)|.$$

From (28), the interpolation error is bounded by

$$|u(x,t) - g(x,t)| \leq \frac{\eta}{2^{N+M}(N+1)!(M+1)!}. \tag{29}$$

We now estimate the second term $|\tilde{u} - g|$. Consider the L^2 norm:

$$\begin{aligned}&\|g(x,t) - \tilde{u}(x,t)\| \\ &= \left(\int_0^1\int_0^1 \left(\sum_{i=0}^{N}\sum_{j=0}^{M}(c_{i,j}p_i(x)p_j(t) - \tilde{c}_{i,j}p_i(x)p_j(t))\right)^2 dxdt\right)^{\frac{1}{2}}.\end{aligned}$$

An application of the Cauchy–Schwarz inequality gives

$$\begin{aligned}&\|g(x,t) - \tilde{u}(x,t)\| \\ &\leq (\sum_{i=0}^{N}\sum_{j=0}^{M}|c_{i,j} - \tilde{c}_{i,j}|^2)^{\frac{1}{2}}(\int_0^1\int_0^1(\sum_{i=0}^{N}\sum_{j=0}^{M}|p_i(x)p_j(t)|)^2 dxdt)^{\frac{1}{2}}.\end{aligned}$$

A simpler bound can be derived by leveraging the orthonormality of the Legendre polynomials (1). Assuming that $\{p_i\}$ are orthonormal gives, results

$$\int_0^1 p_i(x)^2\,dx \le 1.$$

Therefore,

$$\|g(x,t)-\tilde{u}(x,t)\| \le (\sum_{i=0}^{N}\sum_{j=0}^{M}|c_{i,j}-\tilde{c}_{i,j}|^2)^{\frac{1}{2}}\sqrt{NM}.$$

We now find an upper bound for $\sum_{i=0}^{N}\sum_{j=0}^{M}|c_{i,j}-\tilde{c_{i,j}}|$. Let

$$C=[c_{0,0}\cdots c_{N,0}\cdots c_{0,M}\cdots c_{N,M}]^T,$$

and

$$\tilde{C}=[\tilde{c}_{0,0}\cdots \tilde{c}_{N,0}\cdots \tilde{c}_{0,M}\cdots \tilde{c}_{N,M}]^T,$$

where the coefficients $\tilde{c_{i,j}}$ are defined by the orthogonal projection:

$$\tilde{c}_{i,j}=(\frac{1}{\|p_i\|^2\|p_j\|^2}\int_0^1\int_0^1 u(x,t)p_i(x)p_j(t)\,dx\,dt).$$

From the system of equations (21), we obtain

$$C-\tilde{C}=A^{-1}(F-A\tilde{C}),$$

where F is the vector of right-hand side values. Taking norms gives

$$\|C-\tilde{C}\|_2 \le (\|A^{-1}\|_2)\|F-A\tilde{C}\|_2 \le (\|A^{-1}\|_2)\|F-A\tilde{C}\|_\infty.$$

Let $R_{i,j}=(F-A\tilde{C})_{i,j}$ for $i=0,\ldots,N$ and $j=0,\ldots,M$. Then,

$$\begin{aligned}
&|R_{i,j}|\\
&=|(D_t^\alpha g(x_i,t_j)+D_t^\beta g(x_i,t_j)-g_{xx}(x_i,t_j)\\
&\quad+\frac{f(x_i)}{\int_0^1 f(x)dx}(cg(0,t_j)+dg(1,t_j)))-(D_t^\alpha \tilde{u}(x_i,t_j)+D_t^\beta \tilde{u}(x_i,t_j)-\tilde{u}_{xx}(x_i,t_j)\\
&\quad+\frac{f(x_i)}{\int_0^1 f(x)dx}(c\tilde{u}(0,t_j)+d\tilde{u}(1,t_j)))|\\
&\le |D_t^\alpha g(x_i,t_j)-D_t^\alpha \tilde{u}(x_i,t_j)|+|D_t^\beta g(x_i,t_j)-D_t^\beta \tilde{u}(x_i,t_j)|\\
&\quad+|g_{xx}(x_i,t_j)-\tilde{u}_{xx}(x_i,t_j)|\\
&\quad+|\frac{f(x_i)}{\int_0^1 f(x)dx}|\left(|c(g(0,t_j)-\tilde{u}(0,t_j))|+|d(g(1,t_j)-\tilde{u}(1,t_j))|\right).
\end{aligned}$$

Let

$$\vartheta := \max\Big\{\Big|\frac{f(x_i)}{\int_0^1 f(x)\,dx}\Big| : i = 0, 1, \ldots, N\Big\}. \tag{30}$$

Applying Lemma 2 to the error $e(x,t) := u(x,t) - \tilde{u}(x,t)$ and bounding its spatial and temporal derivatives, we obtain estimates of the form

$$\begin{aligned}|R_{i,j}| &\le \frac{\eta}{N^{N-1}M^{M+1}} + \frac{\eta}{N^{N-1}M^{M+1}} + \frac{\eta}{4N^{N-2}M^{M+1}} + \theta\frac{\vartheta(c+d)}{(M+1)!}\\ &\le \frac{3\eta}{N^{N-2}M^{M+1}} + \theta\frac{\vartheta(c+d)}{(M+1)!}.\end{aligned}$$

As a result,

$$\|g(x,t) - \tilde{u}(x,t)\| \le \|A\|_2^{-1}(\sqrt{NM})(\frac{3\eta}{N^{N-2}M^{M+1}} + \theta\frac{\vartheta(c+d)}{(M+1)!}). \tag{31}$$

Finally, combining the estimates (29) and (31), we arrive at the desired result:

$$\begin{aligned}&\sup_{(x,t)\in\Omega} |u(x,t) - \tilde{u}(x,t)|\\ &< \frac{\eta}{2^{N+M}(N+1)!(M+1)!} + (\|A^{-1}\|_2)(\sqrt{NM})(\frac{3\eta}{N^{N-2}M^{M+1}} + \theta\frac{\vartheta(c+d)}{(M+1)!}).\end{aligned}$$

□

6 Numerical examples

In this section, we present the numerical results for two benchmark examples to demonstrate the accuracy, efficiency, and robustness of the proposed shifted-Legendre spectral collocation method. To evaluate the performance of the method, the maximum absolute errors for the state variable $u(x,t)$ and the source term $r(t)$ are defined as follows:

$$\begin{aligned}e_u &= \max_{i,j} |u(x_i,t_j) - u_{N,M}(x_i,t_j)|,\\ e_r &= \max_{j} |r(t_j) - r_{N,M}(t_j)|.\end{aligned}$$

To further investigate the stability and practical applicability of the algorithm, we consider the presence of noise in both the measured data and the model parameters. Furthermore, to assess the convergence behavior of the proposed method, the computational convergence order is determined using the following formula:

$$order \simeq \frac{\log(\frac{e_{N+1}}{e_N})}{\log(\frac{h_{N+1}}{h_N})},$$

where e_{N+1} and e_N denote the maximum absolute errors at two consecutive steps.

In this study, the collocation points are chosen as Chebyshev nodes, defined by

$$x_i = \frac{1}{2}\cos(\frac{(i\pi)}{(N+1)}) + \frac{1}{2}, \quad i = 1, 2, \ldots, N.$$

Since the distance between adjacent points,

$$h_i = x_{i+1} - x_i$$

is nonuniform, we utilize their average value as the effective step length, h_N, for each N. This approach provides a consistent metric for evaluating the rate of convergence across the nonuniform mesh.

Once the numerical solution $\tilde{u}(x,t)$ has been obtained by the proposed method, the approximate source function $\tilde{r}(t)$ is recovered by substituting $\tilde{u}(x,t)$ into (7).

Example 1. Consider the following inverse problem:

$$D_t^{\alpha}u(x,t) + D_t^{\beta}u(x,t) = u_{xx}(x,t) + r(t)\sin(\frac{\pi x}{2} + \frac{\pi}{3}),$$

subject to the initial condition $u(x,0) = 0, \quad x \in [0,1]$, and the boundary conditions:

$$\begin{aligned}
&\tfrac{2}{\sqrt{3}}u(0,t) - 2u(1,t) = 0,\\
&u_x(0,t) - u_x(1,t) - \tfrac{\pi}{2}u(0,t) - \tfrac{\pi}{2}u(1,t) = 0.
\end{aligned}$$

The over-determination data is given by $E(t) = (\frac{\sqrt{3}+1}{\pi})t^3$.

The analytical solution for this problem is

$$u(x,t) = t^3\sin\Big(\frac{\pi x}{2} + \frac{\pi}{3}\Big),$$

and the corresponding exact source function is

$$r(t) = \frac{6}{\Gamma(4-\alpha)}t^{3-\alpha} + \frac{6}{\Gamma(4-\beta)}t^{3-\beta} + \frac{\pi^2}{4}t^3.$$

Table 1 reports the absolute errors and CPU-times for various values of α, β, M, and N using exact data. As shown, the method achieves high precision and efficiency in the absence of noise.

Table 1: Numerical results in Example 1 for different values of α, β, M, and N.

α and β	M and N	CPU-time (sec)	e_u	e_r
$\alpha = 0.9, \beta = 0.2$	$M = 3, N = 5$	1.684024	0.0106	0.0103
	$M = 5, N = 8$	4.694565	6.8791×10^{-6}	7.0042×10^{-6}
	$M = 8, N = 8$	7.540564	6.8788×10^{-6}	7.0033×10^{-6}
$\alpha = 0.5, \beta = 0.8$	$M = 4, N = 5$	2.151800	0.0100	0.0099
	$M = 7, N = 7$	5.527143	3.5097×10^{-5}	1.6260×10^{-4}
	$M = 8, N = 10$	9.783338	4.9522×10^{-8}	5.1959×10^{-8}
$\alpha = 0.4, \beta = 0.6$	$M = 5, N = 7$	4.176156	2.0222×10^{-4}	1.9738×10^{-4}
	$M = 6, N = 9$	6.307603	1.8508×10^{-6}	1.8367×10^{-6}
	$M = 10, N = 12$	16.917430	2.4822×10^{-8}	1.6729×10^{-8}
$\alpha = \beta = 0.5$	$M = N = 10$	13.028037	1.0165×10^{-7}	1.1360×10^{-7}
$\alpha = \beta = 0.9$	$M = N = 10$	12.820756	1.0497×10^{-7}	3.1563×10^{-7}
$\alpha = \beta = 0.3$	$M = N = 10$	12.929664	8.6727×10^{-8}	8.3159×10^{-8}

Figure 1 illustrates the absolute error of $u(x,t)$ for various fractional orders. To evaluate the reconstruction of the unknown source term, Figure 2 displays the comparison between the exact function $r(t)$ and its numerical approximation $\tilde{r}(t)$. It is evident that the two curves are indistinguishable, and the absolute error remains near the machine precision level, confirming the high fidelity of the spectral approach.

To further investigate the stability and practical applicability of the method, we test its sensitivity to data perturbations. In real-world inverse problems, the observed data are often corrupted by measurement errors. Therefore, to simulate real-world measurement uncertainties, a certain level of random noise is added to the additional integral condition and the coefficients associated with the nonlocal boundary conditions. So, the right-hand side vector in (21) is contaminated with noise, which is modeled as follows:

$$\mathcal{F}^{\epsilon} = \mathcal{F} + \epsilon(2.rand(S) - 1),$$

where ϵ represents the noise level, S is the dimension of $\mathcal{F}$ and $rand()$ generates uniformly distributed random numbers on $[0,1]$.

As observed in Table 2, even with significant noise levels in $\mathcal{F}$, the method remains stable. Furthermore, as M and N increase, the error does not grow significantly and stays within a consistent range, demonstrating that the proposed technique is robust against numerical instabilities and does not suffer from ill-conditioning in the presence of perturbations.

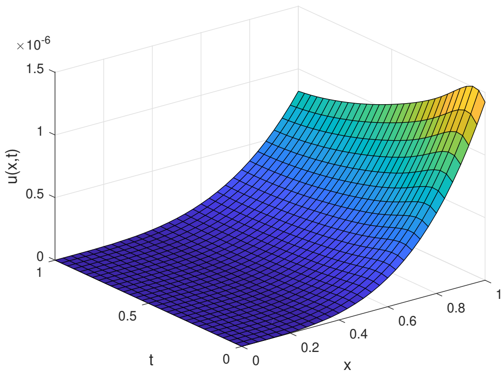

(a) $\alpha = 0.9, \beta = 0.2$, and $M = N = 8$.

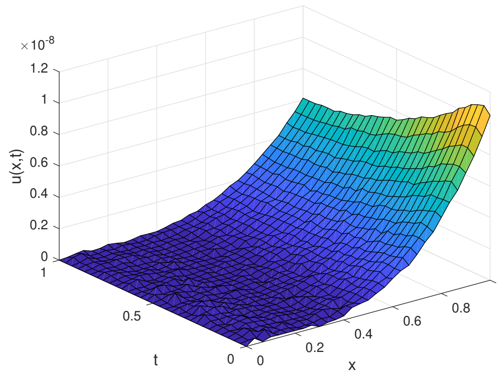

(b) $\alpha = 0.5, \beta = 0.8$, $M = 8$, and $N = 10$.

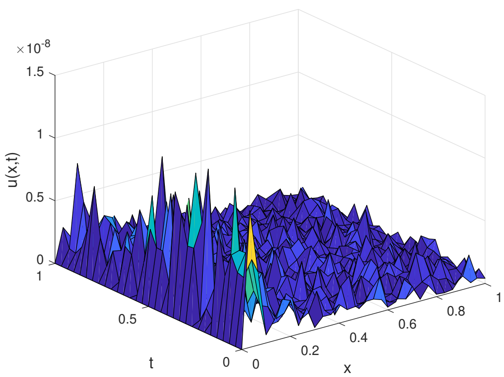

(c) $\alpha = 0.4, \beta = 0.6$, $M = 10$, and $N = 12$.

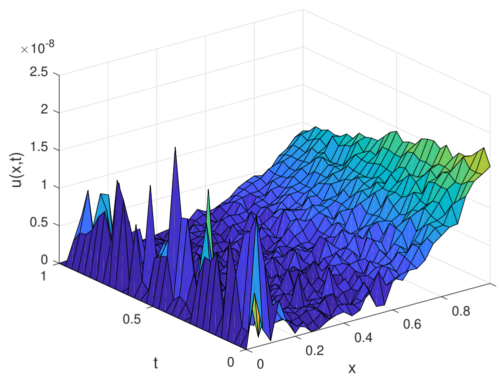

(d) $\alpha = \beta = 0.3$ and $M = N = 10$.

Figure 1: Absolute errors in Example 1.

Table 2: Numerical results for Example 1 in the presence of noise when $\alpha = 0.2$ and $\beta = 0.9$.

	$\epsilon = 0.005$	$\epsilon = 0.01$	$\epsilon = 0.05$	$cond(A)$
$N = 5$	$\|\|u_\epsilon\|\|_\infty = 0.2341$	$\|\|u_\epsilon\|\|_\infty = 0.1126$	$\|\|u_\epsilon\|\|_\infty = 0.2168$	3.2101×10^4
$M = 5$	$\|\|r_\epsilon\|\|_\infty = 0.1115$	$\|\|r_\epsilon\|\|_\infty = 0.7081$	$\|\|r_\epsilon\|\|_\infty = 0.6911$	
$N = 7$	$\|\|u_\epsilon\|\|_\infty = 0.0201$	$\|\|u_\epsilon\|\|_\infty = 0.3161$	$\|\|u_\epsilon\|\|_\infty = 0.5160$	9.8523×10^4
$M = 6$	$\|\|r_\epsilon\|\|_\infty = 0.3686$	$\|\|r_\epsilon\|\|_\infty = 0.2395$	$\|\|r_\epsilon\|\|_\infty = 0.9997$	
$N = 8$	$\|\|u_\epsilon\|\|_\infty = 0.0252$	$\|\|u_\epsilon\|\|_\infty = 0.0578$	$\|\|u_\epsilon\|\|_\infty = 0.1584$	2.2732×10^5
$M = 6$	$\|\|r_\epsilon\|\|_\infty = 0.0648$	$\|\|r_\epsilon\|\|_\infty = 0.1316$	$\|\|r_\epsilon\|\|_\infty = 0.4501$	

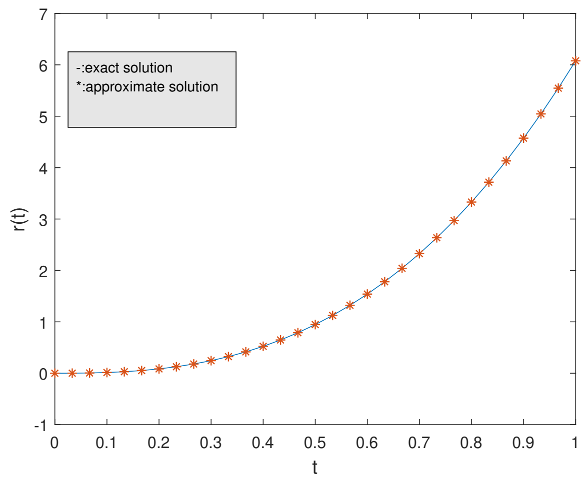

Figure 2: Comparison between the exact and approximate values of $r(t)$ in Example 1.

It is important to note that while the discrete system matrix exhibits a relatively high condition number, the stability of the obtained results is consistent with the theoretical well-posedness of the underlying inverse problem. Therefore, the proposed numerical procedure maintains its reliability and produces stable solutions without the necessity of any additional regularization techniques.

Furthermore, to demonstrate the method's performance under measurement errors, Figure 3 presents the numerical results in the presence of several noise levels for $\alpha = 0.2$ and $\beta = 0.9$. This figure shows the three-dimensional error distribution of $u(x,t)$, along with the reconstructed source term. Despite the noise, the method maintains stable behavior, and no oscillations are observed in the reconstructed source function.

Example 2. Consider the problem (1)–(5) with the exact solution $u(x,t) = t^2 e^{2x+1}$ and the source term

$$r(t) = \frac{\Gamma(3)}{\Gamma(3-\alpha)} t^{2-\alpha} + \frac{\Gamma(3)}{\Gamma(3-\beta)} t^{2-\beta} - 4t^2.$$

The initial condition is $u_0(x) = 0$, and the coefficients in the nonlocal boundary conditions are $a = e^2, b = -1, c = -2$, and $d = 2$.

Table 3 reports the maximum absolute errors for both $u(x,t)$ and $r(t)$, alongside the CPU-time for various values of M, N, α and β. The results in this table indicate that the method achieves high accuracy even with a small number of collocation points. For instance, when $\alpha = 0.1, \beta = 0.3$ and $M = N = 9$, the error in u reaches as low as 4.52×10^{-7}.

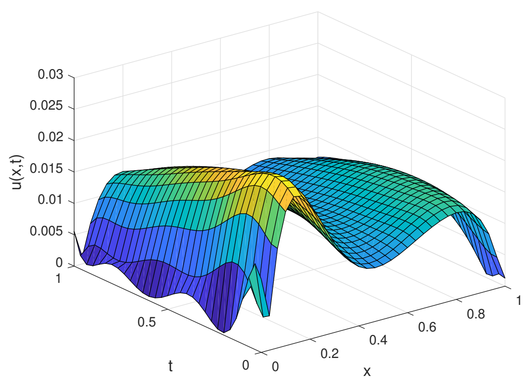

(a)

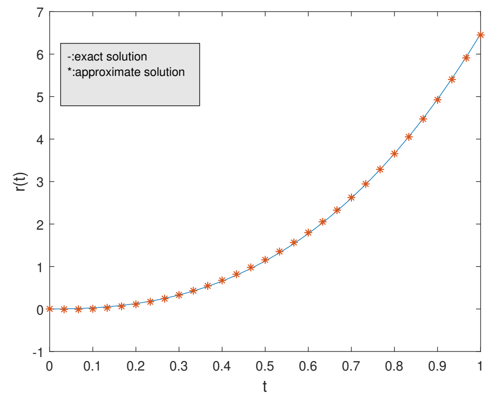

(b)

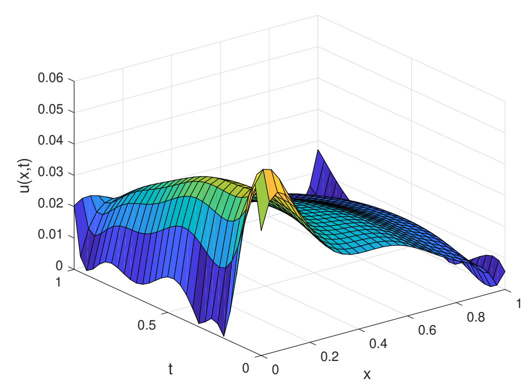

(c)

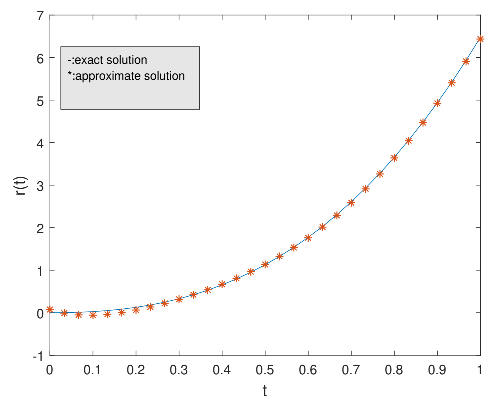

(d)

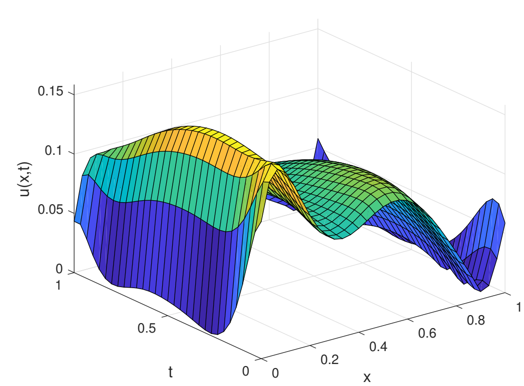

(e)

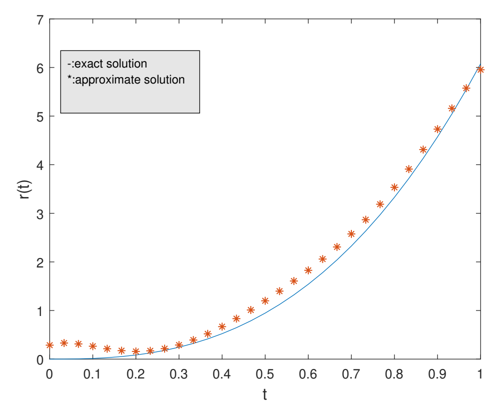

(f)

Figure 3: The absolute errors of $u(x,t)$ (left), and the reconstructed source term $r(t)$ (right) in Example 1 under different noise levels, $\epsilon = 0.005$ (first row), $\epsilon = 0.01$ (second row), and $\epsilon = 0.05$ (third row) when $\alpha = 0.2$, $\beta = 0.9$, $M = 6$, and $N = 8$.

Table 3: Numerical results in Example 2 for different values of α, β, M, and N.

α and β	M and N	CPU time (sec)	error of $u(x,t)$	error of $r(t)$
$\alpha=0.2, \beta=0.9$	$M=5, N=8$	4.872626	0.0025	3.1055×10^{-4}
	$M=6, N=9$	6.131564	2.8945×10^{-4}	3.6336×10^{-5}
	$M=9, N=10$	17.587541	3.0142×10^{-5}	3.7863×10^{-6}
$\alpha=0.1, \beta=0.3$	$M=N=4$	1.914168	0.0058	0.5103
	$M=N=6$	3.997282	1.5651×10^{-4}	0.0236
	$M=N=9$	9.213205	4.5291×10^{-7}	5.5964×10^{-5}
$\alpha=0.1, \beta=0.3$	$M=5, N=8$	4.462392	0.0040	4.8001×10^{-4}
	$M=6, N=9$	5.912642	4.6522×10^{-4}	5.5962×10^{-5}
	$M=9, N=10$	10.421637	4.8439×10^{-5}	5.8361×10^{-6}
$\alpha=\beta=0.5$	$M=N=8$	7.008119	0.0028	3.5138×10^{-4}
$\alpha=\beta=0.8$	$M=N=8$	6.849998	0.0020	2.5458×10^{-4}
$\alpha=\beta=0.2$	$M=N=8$	6.719837	0.0040	4.8212×10^{-4}

To visualize the accuracy of the proposed method for Example 2, Figure 4 displays the three-dimensional absolute error surfaces of $u(x,t)$ for different fractional orders and collocation points. The smooth and low-magnitude error surfaces confirm the uniform convergence of the method. Additionally, Figure 5 provides a comparison between the exact source term $r(t)$ and its numerical reconstruction $\tilde{r}(t)$. The perfect overlap between the two curves, along with the negligible absolute error, demonstrates the high precision of the method in identifying the unknown source term.

To further investigate the convergence behavior, Table 4 summarizes the numerical convergence orders for $\alpha = 0.2$ and $\beta = 0.9$. It is evident that the convergence order increases significantly as N increases, which is a typical characteristic of spectral methods, demonstrating that the proposed approach is far more efficient than low-order finite difference schemes.

Table 4: Numerical convergence orders in Example 2 when $\alpha = 0.2$ and $\beta = 0.9$.

$M=N$	h_N	*error*	*order*
5	0.2165	0.7010	
6	0.1802	0.1216	9.6187
7	0.15398	0.0188	12.1186
8	0.13423	0.0025	15.0754
9	0.11888	2.8936×10^{-4}	18.2925
10	0.10661	3.0180×10^{-5}	21.4752

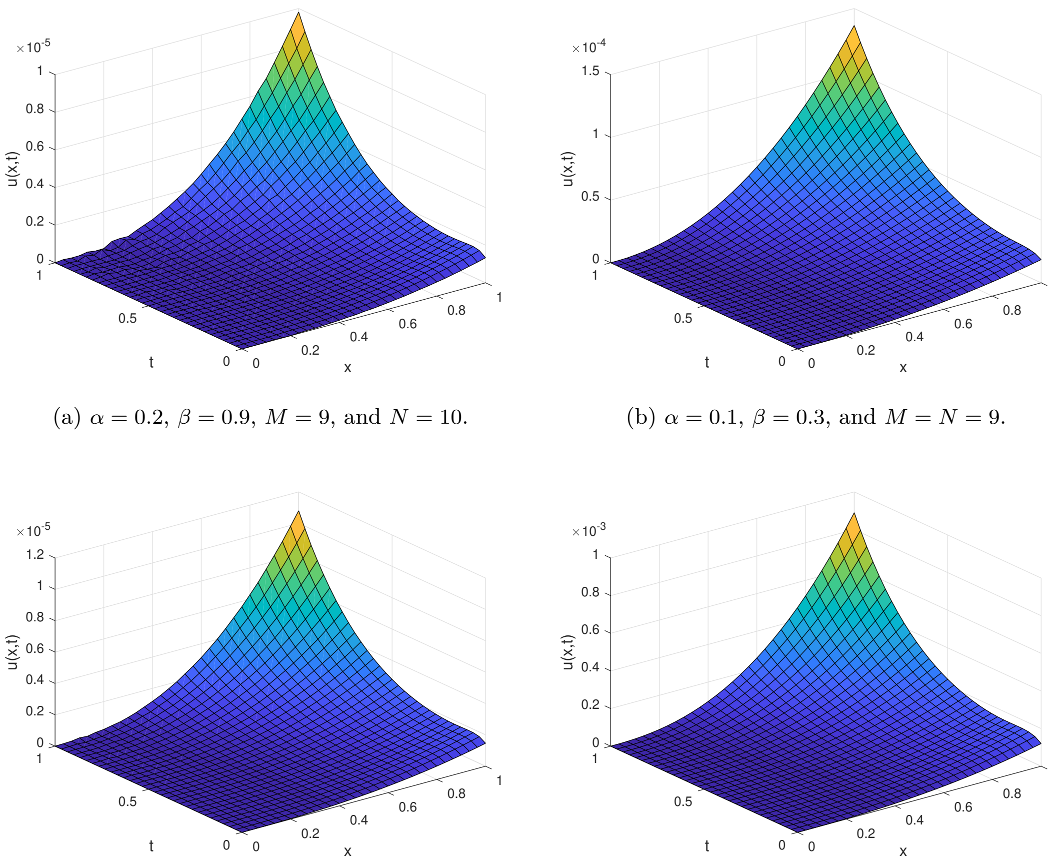

(a) $\alpha = 0.2$, $\beta = 0.9$, $M = 9$, and $N = 10$.

(b) $\alpha = 0.1$, $\beta = 0.3$, and $M = N = 9$.

(c) $\alpha = 0.4$, $\beta = 0.6$, $M = 9$, and $N = 10$.

(d) $\alpha = \beta = 0.5$ and $M = N = 8$.

Figure 4: Absolute error distribution in Example 2 for various values of α, β, M, and N.

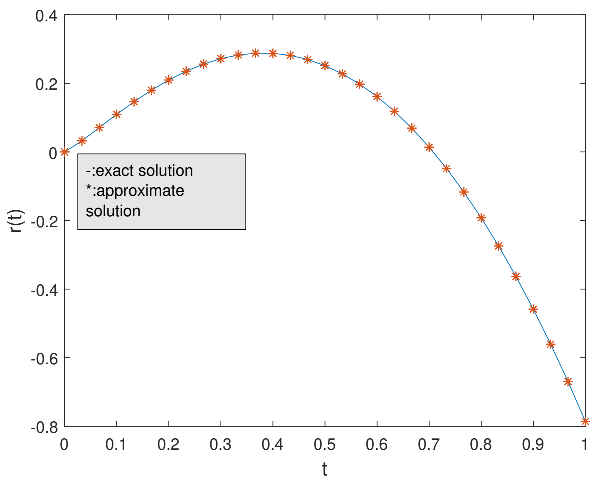

Figure 5: Comparison between the exact and recovered source terms $r(t)$ for Example 2.

In addition, to provide a visual representation of the method's stability, Figure 6 illustrates the absolute error distribution of the numerical solution and the recovered source term in the presence of different noise levels. Despite the perturbation in the data, the error surfaces remain smooth and free of any numerical oscillations.

The sensitivity of the method to noisy data is analyzed in Table 5. As observed in this table, although the condition number $cond(A)$ increases with N, the absolute errors for both the state variable and the source term remain controlled.

Table 5: Numerical results for Example 2 in the presence of various noise levels with $\alpha = 0.4$ and $\beta = 0.8$.

	$\epsilon = 0.01$	$\epsilon = 0.05$	$\epsilon = 0.1$	$cond(A)$
$N = 4$	$\|\|u_\epsilon\|\|_\infty = 0.8122$	$\|\|u\epsilon\|\|_\infty = 0.7271$	$\|\|u_\epsilon\|\|_\infty = 0.5685$	1.2624×10^3
$M = 4$	$\|\|r_\epsilon\|\|_\infty = 0.1640$	$\|\|r_\epsilon\|\|_\infty = 0.1661$	$\|\|r_\epsilon\|\|_\infty = 0.1910$	
$N = 6$	$\|\|u_\epsilon\|\|_\infty = 0.3273$	$\|\|u_\epsilon\|\|_\infty = 0.2255$	$\|\|u_\epsilon\|\|_\infty = 0.3415$	1.0221×10^5
$M = 6$	$\|\|r_\epsilon\|\|_\infty = 0.208$	$\|\|r_\epsilon\|\|_\infty = 0.0928$	$\|\|r_\epsilon\|\|_\infty = 0.2154$	
$N = 8$	$\|\|u_\epsilon\|\|_\infty = 0.0589$	$\|\|u_\epsilon\|\|_\infty = 0.2812$	$\|\|u_\epsilon\|\|_\infty = 1.0841$	2.2918×10^5
$M = 6$	$\|\|r_\epsilon\|\|_\infty = 0.0119$	$\|\|r_\epsilon\|\|_\infty = 0.0592$	$\|\|r_\epsilon\|\|_\infty = 1.0841$	

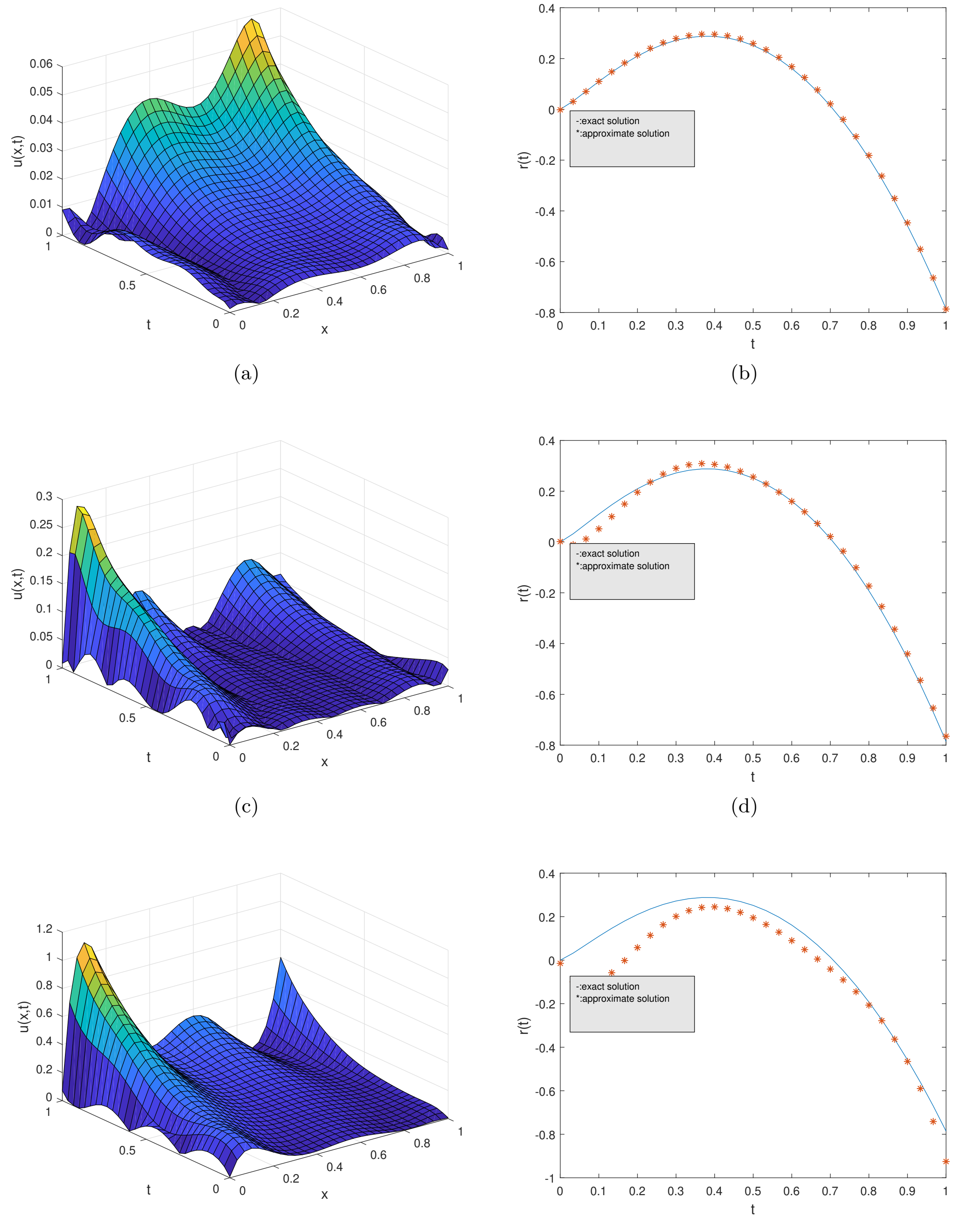

(a) (b)

(c) (d)

(e) (f)

Figure 6: The absolute errors of $u(x,t)$ (left), and the reconstructed source term $r(t)$ (right) in Example 2 under different noise levels, $\epsilon = 0.01$ (first row), $\epsilon = 0.05$ (second row), and $\epsilon = 0.1$ (third row) with $\alpha = 0.4$, $\beta = 0.8$, $M = 6$, and $N = 8$.

7 Conclusion

An efficient spectral collocation method based on shifted Legendre polynomials has been developed for the numerical solution of an inverse source problem for two-term time-fractional diffusion equations subject to nonlocal boundary conditions. The proposed approach successfully reconstructs the unknown time-dependent source term $r(t)$ while simultaneously approximating the solution $u(x,t)$. A rigorous convergence analysis has been carried out, establishing optimal error estimates under standard regularity assumptions. The theoretical results are validated through extensive numerical experiments on benchmark problems, which demonstrate the spectral accuracy and rapid convergence of the proposed method with respect to the collocation parameters N and M. Moreover, the unknown source function $r(t)$ is recovered with high accuracy.

In summary, the proposed method is accurate, stable, and straightforward to implement. These features make it a reliable and competitive numerical technique for solving inverse problems arising in multi-term fractional diffusion models with nonlocal constraints.

Funding

This research received no external funding.

Conflicts of Interest

The authors declare no conflicts of interest.

Acknowledgments

We are also grateful to the Editor and the anonymous reviewers for their constructive comments and suggestions that significantly improved the quality of this manuscript.

References

[1] Abdollahi, N. and Rostamy, D. *Identifying an unknown time-dependent boundary source in time-fractional diffusion equation with a non-local boundary condition*, J. Comput. Appl. Math., 355 (2019), 36–50.

[2] Ali, M. and Aziz, S. *Some inverse problems for time-fractional diffusion equation with nonlocal Samarskii–Ionkin type condition*, Math. Methods Appl. Sci., 44 (2021), 8447–8462.

[3] Arridge, S., Maas, P., Öktem, O. and Schönlieb, C.B. *Solving inverse problems using data-driven models*, Acta Numer., 28 (2019), 1–174.

[4] Bazan, F., Bedin, L., Ismailov, M.I. and Borges, L. *Inverse time-dependent source problem for the heat equation with a nonlocal Wentzell–Neumann boundary condition*, Netw. Heterog. Media, 18 (2023), 1747–1771.

[5] Beckers, S. and Yamamoto, M. *Regularity and unique existence of solution to linear diffusion equation with multiple time-fractional derivatives*, In *Control and Optimization with PDE Constraints*, Springer, (2013), 45–55.

[6] Błasik, M. *Numerical scheme for a two-term sequential fractional differential equation*, Sci. Res. Inst. Math. Comput. Sci., 10(2) (2011), 17–29.

[7] Brandibur, O. and Kaslik, É. *Stability properties of multi-term fractional-differential equations*, Fractal Fract., 7(2) (2023), 117.

[8] Chen, J., Liu, F. and Anh, V. *Analytical solution for the time-fractional telegraph equation by the method of separating variables*, J. Math. Anal. Appl., 338(2) (2008), 1364–1377.

[9] Chung, J. and Gazzola, S. *Computational methods for large-scale inverse problems: a survey on hybrid projection methods*, SIAM Rev., 66(2) (2024), 205–284.

[10] D'Abbicco, M. and Girardi, G. *Asymptotic profile for a two-terms time fractional diffusion problem*. Fract. Calc. Appl. Anal. 25(3) (2022), 1199–1228.

[11] D'Abbicco, M. and Girardi, G. *Decay estimates for a perturbed two-terms space-time fractional diffusive problem*, Evol. Equ. Control Theory, 12(4) (2023), 1106–1138.

[12] Derbissaly, B., Kirane, M. and Sadybekov, M.A. *Inverse source problem for two-term time-fractional diffusion equation with nonlocal boundary conditions*, Chaos Solitons Fractals, 183 (2024), 114897.

[13] Dib, F. and Kirane, M. *An inverse source problem for a two terms time-fractional diffusion equation*, Bol. Soc. Parana. Mat., 2022 (2022) 1–15.

[14] Ding, M.H., Liu, H. and Lo, C.W. *Inverse problems for coupled nonlocal nonlinear systems arising in mathematical biology*, arXiv preprint arXiv:2407.15713, 2024.

[15] Fazli, H., Bahrami, F. and Shahmorad, S. *Extremal solutions for multi-term nonlinear fractional differential equations with nonlinear boundary conditions*, Comput. Methods Differ. Equ., 11(1) (2023), 32–41.

[16] Furati, K.M., Iyiola, O.S. and Kirane, M. *An inverse problem for a generalized fractional diffusion*, Appl. Math. Comput., 249 (2014), 24–31.

[17] Hazanee, A., Lesnic, D., Ismailov, M.I. and Kerimov, N.B. *Inverse time-dependent source problems for the heat equation with nonlocal boundary conditions*, Appl. Math. Comput., 346 (2019), 800–815.

[18] Ismailov, M.I. *Inverse source problem for heat equation with nonlocal Wentzell boundary condition*, Results Math., 73(2) (2018) 68.

[19] Ismailov, M.I. and Cicek, M. *Inverse source problem for a time-fractional diffusion equation with nonlocal boundary conditions*, Appl. Math. Model., 40 (2016), 4891–4899.

[20] Ismailov, M.I. and Tekin, I. *An inverse problem for finding the lowest term of a heat equation with Wentzell–Neumann boundary condition*, Inverse Probl. Sci. Eng., 27 (2019), 1608–1634.

[21] Jafari, H., Babaei, A. and Banihashemi, S. *A novel approach for solving an inverse reaction–diffusion–convection problem*, J. Optim. Theory Appl., 183 (2019), 688–704.

[22] Khosravian-Arab, H. and Dehghan, M. *A matrix approach to multi-term fractional differential equations using two new diffusive representations for the Caputo fractional derivative*, AUT J. Math. Comput., 5(4) (2024), 337–359.

[23] Kilbas, A.A., Srivastava, H.M. and Trujillo, J.J. *Theory and applications of fractional differential equations*, Elsevier, 2006.

[24] Kirane, M., Malik, S.A. and Al-Gwaiz, M.A. *An inverse source problem for a two dimensional time fractional diffusion equation with nonlocal boundary conditions*, Math. Methods Appl. Sci., 36(9) (2013), 1056–1069.

[25] Kirane, M., Sadybekov, M.A. and Sarsenbi, A.A. *On an inverse problem of reconstructing a subdiffusion process from nonlocal data*, Math. Methods Appl. Sci., 42 (2019), 2043–2052.

[26] Lattanzi, A.M. and Hrenya, C.M. *A coupled, multiphase heat flux boundary condition for the discrete element method*, Chem. Eng. J., 304 (2016), 766–773.

[27] Li, T.-T. *A class of non-local boundary value problems for partial differential equations and its applications in numerical analysis*, J. Comput. Appl. Math., 28 (1989), 49–62.

[28] Li, Y., Wang, T. and Gao, G.H. *The asymptotic solutions of two-term linear fractional differential equations via Laplace transform*, Math. Comput. Simul., 211 (2023), 394–412.

[29] Ma, R. *A survey on nonlocal boundary value problems*, Appl. Math. E-Notes, 7 (2007), 257–279.

[30] Malik, S.A. and Aziz, S. *An inverse source problem for a two parameter anomalous diffusion equation with nonlocal boundary conditions*, Comput. Math. Appl., 73(12) (2017), 2548–2560.

[31] Nemati, S. and Babaei, A. *A numerical method based on the Jacobi polynomials to reconstruct an unknown source term in a time fractional diffusion-wave equation*, Taiwanese J. Math., 23(5) (2019), 1271–1289.

[32] Orazov, I. and Makhatova, A.K. *On application of inverse problems with the nonlocal boundary conditions in the diffusion theory*, In *International Conference "Functional Analysis in Interdisciplinary Applications" (FAIA2017)*, Vol. 1880, AIP Publishing, (2017), 060008.

[33] Orazov, I. and Sadybekov, M.A. *On a class of problems of determining the temperature and density of heat sources given initial and final temperature*, Sib. Math. J., 53(1) (2012), 146–151.

[34] Orsingher, E. and Beghin, L. *Time-fractional telegraph equations and telegraph processes with Brownian time*, Probab. Theory Relat. Fields, 128(1) (2004), 141–160.

[35] Ozkan, A.S. and Adalar, İ. *Inverse nodal problems for Sturm–Liouville equation with nonlocal boundary conditions*, J. Math. Anal. Appl., 520(1) (2023), 126904.

[36] Pal, S. and Melnik, R. *Nonlocal models in biology and life sciences: sources, developments, and applications*, arXiv preprint arXiv:2401.14651, 2024.

[37] Rivlin, T.J. *Chebyshev polynomials*, Courier Dover Publications, 2020.

[38] Sadybekov, M.A. and Pankratova, I.N. *Correct and stable algorithm for numerical solving nonlocal heat conduction problems with not strongly regular boundary conditions*, Mathematics, 10(20) (2022), 3780.

[39] Stojanović, M. *Existence–uniqueness result for a nonlinear n-term fractional equation*, J. Math. Anal. Appl., 353(1) (2009), 244–255.

[40] Stojanović, M. and Gorenflo, R. *Nonlinear two-term time fractional diffusion-wave problem*, Nonlinear Anal. Real World Appl., 11(5) (2010), 3512–3523.

[41] Sun, L.L. and Yan, X.B. *Inverse source problem for a multiterm time-fractional diffusion equation with nonhomogeneous boundary condition*, Adv. Math. Phys., 2020 (2020), 1825235.

[42] Vogel, C.R. *Computational methods for inverse problems*, Soc. Ind. Appl. Math., 2002.

[43] Yadigaroglu, G. and Hewitt, G.F. *Introduction to multiphase flow: basic concepts, applications and modelling*, Springer, 2017.

[44] Zhou, Y. and He, J.W. *Well-posedness and regularity for fractional damped wave equations*, Monatsh. Math., 194 (2021), 425–458.